BIREFRINGENCE AND 7CB LIQUID CRYSTAL ALIGNMENT IN PVA FILMS FROM UV-IRRADIATED SOLUTIONS

Cristina-Delia NECHIFOR [1*], Marian LUȚCANU [2]

This study examines UV irradiation (0–20 min) and uniaxial stretching ($\gamma = 1.5, 2$) effects on polyvinyl alcohol (PVA) films from UV-irradiated solutions, optimizing birefringence and 7CB liquid crystal (LC) alignment. At 10 min UV, photooxidation enhances polarity ($P = 35.6 \pm 0.62\%$), wettability ($\Delta G_w = -123.48 \pm 0.48\, mJ/m^2$), and birefringence ($\Delta n = 0.00434$, unstretched) via intramolecular hydrogen bonding. Crosslinking at 15–20 min reduces polarity and smoothness. Stretching boosts birefringence, peaking at $\gamma = 1.5$ for 10-min UV films ($\Delta n = 0.03092$). Optimal 7CB alignment ($R_{Bright/Dark} = 7.16$) occurs at 10 min UV and $\gamma = 1.5$, enabling tailored PVA films for polarizers and LC displays.

Keywords: Polyvinyl alcohol (PVA), UV irradiation, mechanical stretching, optical birefringence, surface polarity, liquid crystal (LC) alignment, 7CB.

1. Introduction

Polyvinyl alcohol (PVA) is a versatile polymer widely used in optical and liquid crystal (LC) alignment applications due to its excellent film-forming ability, optical transparency, and hydrophilicity from hydroxyl (OH) groups [1]. These properties make PVA films ideal for polarizers, optical filters, and LC alignment layers, where high birefringence and uniform LC orientation are critical [1, 2]. The performance of PVA films depends on their molecular structure, surface chemistry, and structural order, which can be tailored through modification techniques such as irradiation and mechanical stretching [3-6].

UV irradiation induces photochemical reactions in PVA, including chain scission, photooxidation, and crosslinking, generating polar carbonyl ($C = O$) and OH groups that enhance surface polarity, wettability, and chain mobility [3,4, 7-9]. These changes promote intramolecular hydrogen bonding and ordered chain packing, increasing optical birefringence, but prolonged exposure forms ether ($C - O - C$) and ester ($-COO-$) bridges, increasing rigidity and surface roughness, which may impair optical clarity and LC alignment [7, 8]. Mechanical stretching aligns PVA chains along the deformation axis, enhancing crystallinity,

* Corresponding author
[1] Lecturer, Dept. of Physics, "Gheorghe Asachi" Technical University of Iași, Romania, e-mail: cristina-delia.nechifor@academic.tuiasi.ro
[2] Eng., Dept. of Physics, "Gheorghe Asachi" Technical University of Iași, Romania, e-mail: marian.lutcanu@staff.tuiasi.ro

birefringence, and surface anisotropy, while reorienting polar groups to modulate LC adhesion [6, 10].

Although UV irradiation and stretching individually enhance PVA properties, their combined effects on optical birefringence, surface characteristics, and 7CB LC alignment remain underexplored, particularly regarding the balance between hydrogen bonding, crosslinking, and chain orientation [4-10]. This knowledge gap is critical for LC alignment, where surface polarity [12-13] enhances adhesion through intermolecular interactions, while surface anisotropy [14] primarily drives molecular orientation for nematic LC like 7CB [15].

This study investigates the synergistic effects of UV irradiation (0, 10, 15, 20 minutes) and uniaxial stretching ($\gamma = 1.5$ and 2) on PVA films, focusing on their optical birefringence, surface polarity, wettability, and 7CB LC alignment. Films were characterized using polarized optical microscopy (POM), ATR-FTIR spectroscopy, contact angle measurements, and birefringence analysis to elucidate molecular mechanisms, including photooxidation-driven hydrogen bonding at shorter exposures and crosslinking at longer ones.By correlating these properties with UV exposure and stretching degree, this work provides a framework for optimizing PVA films for photonic applications, advancing polymer surface engineering for polarizers and LC displays.

2. Materials and Methods:

Materials: Polyvinyl alcohol (PVA, 99+% hydrolysed, Mw = 89.000-98.000, Sigma-Aldrich) was dissolved in distilled water at $90\ °C$ with stirring for 12 hours to prepare $10\ wt.\%$ PVA solutions. Diiodomethane and 4-cyano-4'-heptylbiphenyl (7CB, Sigma-Aldrich) were used as received.

PVA ($-[CH_2 - CH(OH)]_n-$) is a water-soluble polymer with hydroxyl groups enabling intramolecular hydrogen bonding, with a glass transition temperature ($T_g = 75 - 85°C$) and melting point ($T_m = 250$°C). 7CB ($C_{20}H_{23}N$) has a cyanobiphenyl structure with a heptyl chain and positive dielectric anisotropy ($\Delta\varepsilon = 8$ at $25°C$). The 7CB transitions from crystalline to SmA is at $\sim 30\ °C$ and SmA to nematic at $\sim 30.2 - 30.5\ °C$, with the nematic phase stable up to $42.8\ °C$, [15, 16].]. To ensure fully nematic behaviour and avoid smectic contamination, all POM measurements were conducted at $32\ °C$, using a thermostated stage with a thermal inertia of ±2 °C, resulting in an actual sample temperature range of $30 - 32\ °C$ during stable operation.

Samples preparation: PVA solutions (60 mL) were UV-irradiated in quartz vessels (13 cm² area) using a high-pressure mercury lamp (Hg-50W, arc length 1 mm, quartz lens) at 10 cm distance for 0, 10, 15, and 20 minutes, delivering doses of 5.77, 8.66, and $11.54\ J/cm^2$ at an intensity of $9.62\ mW/cm^2$. Irradiated solutions were cast onto cleaned glass plates (23 cm X 23 cm) and dried at $27°C$

for three days in a covered enclosure to minimize dust contamination. The resulting films were cut into standard tensile test specimens (bone shape) having gauge length 4 cm and width 3 cm. Films were clamped at both ends using custom-made stainless-steel grips with a 4 cm initial gauge length. Each film was then heated to 42–45 °C (below T_g) for 5 min on a thermostated oven to enhance chain mobility without inducing flow. Uniaxial stretching was performed manually at a constant rate of $\approx\ 2\ mm/s$ until the desired draw ratio ($\gamma\ =\ 1.5$or 2)was achieved. The draw ratio γ was defined as the ratio of the major to minor semi-axis of an ellipse formed from an initially circular mark ($\emptyset\ =\ 2\ cm$) drawn on the film surface prior to stretching [1]. After reaching the target γ, the stretched films were held under tension for $10\ min$ and slowly cooled to room temperature while maintaining the clamps to lock in the oriented structure. Films ($0.8-0.9\ mm$ thick) were stored in a desiccator with silica gel at $25\pm2°C$ for 1–3 days to prevent moisture absorption before characterization.

Characterization: PVA film thickness was measured at 10 points using a micrometre screw gauge, with average thicknesses ranging from 0.8 to $0.9\ mm$. Only films within this range were used due to their enhanced tensile strength and resistance to deformation during stretching compared to thinner films.

Structural changes in PVA films before and after UV irradiation were analysed using Attenuated Total Reflectance Fourier Transform Infrared (ATR-FTIR) spectroscopy on a Bruker Vertex 70 spectrometer (Bruker Optik GmbH, Ettlingen, Germany).

Surface morphology of unstretched PVA films was examined using Scanning Electron Microscopy (SEM) with a FEI Quanta 200 SEM (FEI Company, Brno, Czech Republic).

Optical birefringence (Δn) of PVA films was measured using the light polarization ellipse method [11] with a sodium lamp ($\lambda = 589.3\ nm$), two polarizers, and a silicon-based photodetector ($390-1150\ nm$, PHYWE, Göttingen, Germany). The first polarizer was rotated to select an azimuth angle ($\alpha\ =\ 10°$ to 43°), and the second polarizer was adjusted to maximize luminous flux, recording the angle (θ). Birefringence was calculated using Equation (1), see Fig.1 for the experimental setup, where l is film thickness:

$$\Delta n\ =\ \lambda/(2\pi l)\ arccos(\frac{tan2\theta}{tan2\alpha}) \quad (1)$$

Five α values were measured per film, and the average Δn was calculated with a relative error of 2.15% ($\Delta\lambda = 0.6\ nm, \Delta l = 1\ \mu m, \Delta\theta = \Delta\alpha = 0.01°$).

Contact angles of water and diiodomethane were measured at $25\pm2°C$ using a KSV CAM 101 system (KSV Instruments Ltd., Helsinki, Finland). The sessile drop method used $\sim5\ \mu l$ droplets, with five measurements at three regions per film (accuracy: 1°). Contact angles were recorded after 10s stabilization, and average values with relative errors were calculated.

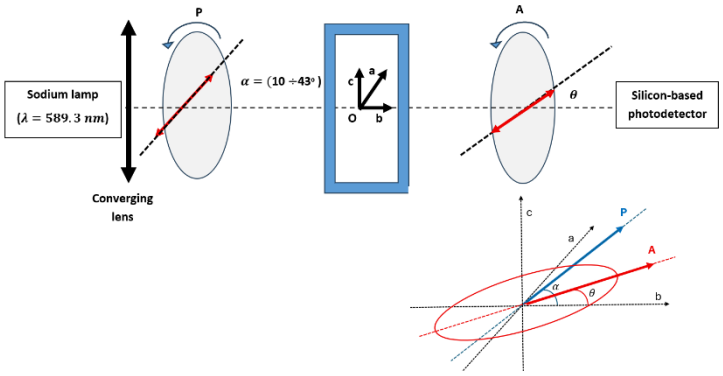

Fig. 1. The polarization ellipse method for measuring optical birefringence. The incident light is polarized at angle α; the analyzer is rotated to θ to maximize intensity. The phase difference induces an elliptical polarization state, from which Δn is calculated using Equation (1).

The alignment of 7CB nematic LC on pristine and stretched PVA films was evaluated using polarizing optical microscopy (POM) on a Carl Zeiss Jena Amplival microscope (Carl Zeiss, Jena, Germany) at $32°C$ to ensure the nematic phase. A small droplet (0.5 µL) of LC layer was deposited on the PVA-coated glass substrate (single plate, not sandwiched) and gently covered with a coverslip to form a non-confined layer was applied. This open configuration allows direct evaluation of surface-induced alignment without bulk confinement effects. The sample was heated to $40\,°C$, then gradually cooled to 32 °C to promote uniform planar alignment from the PVA surface. The 32x magnified images were acquired under crossed polarizers.

ImageJ software (National Institutes of Health, USA) quantified brightness by converting POM images to grayscale (0–255 intensity). Regions of interest (ROIs) were defined over bright and dark textures, and average intensities were calculated from histograms [17]. The contrast ratio ($R_{Bright/Dark}$) was determined using Equation (2):

$$R_{Bright/Dark} = \frac{I_{Bright}}{I_{Dark}} \tag{2}$$

where I_{Bright} and I_{Dark} are average intensities of bright and dark states, respectively. Precision was assessed using the standard error propagation method, with relative error derived from standard deviation across five ROIs per image.

3. Results and Discussion

The effects of UV exposure on the chemical, optical, and surface properties of cast PVA films prepared from UV-irradiated aqueous solutions were analysed and discussed. The films were then subjected to uniaxial stretching, and the effects of this mechanical post-treatment on their birefringence, surface polarity, and LCs alignment on the stretched film surfaces were assessed.

3.1. Spectral Analysis of PVA Films Prepared from UV Irradiated PVA Aqueous Solutions

Structural characterization of the PVA films was performed using ATR-FTIR spectroscopy. Fig. 2 shows the ATR-FTIR spectra of films prepared from unexposed and UV-irradiated PVA solutions, highlighting the major peaks associated with PVA.

The spectra reveal the OH stretching vibration with strong hydrogen bonding ($\upsilon = 3300\ cm^{-1}$), with peak intensity decreasing with UV exposure time due to oxidation or loss of hydroxyl groups through photodegradation. The $C-H$ asymmetric stretch (CH_2, $\upsilon = 2900-2950\ cm^{-1}$) and symmetric stretch (CH_2, $\upsilon = 2850-2900\ cm^{-1}$) exhibit a slight decrease in intensity with UV exposure [18]. The C=O stretching peak ($\upsilon = 1730\ cm^{-1}$) in the pristine film spectra is attributed to residual carbonyl groups from incomplete vinyl acetate polymerization [19]. Additional peaks at $\upsilon = 1420\ cm^{-1}$ ($C-H$ bending vibration of the CH_2 groups within the polymer backbone), $\upsilon = 1330\ cm^{-1}$ ($C-H$ wagging vibration of the CH_2 groups within the polymer chain.), $\upsilon = 1142\ cm^{-1}$ (CH_2wagging and OH bending), $\upsilon = 1088\ cm^{-1}$ ($C-O$ stretch of hydroxyl-bearing carbon, influenced by hydrogen bonding), and $\upsilon = 840\ cm^{-1}$ (CH rocking) are characteristic of PVA [18]. No changes were observed in the bands from 1660 to 1570 cm^{-1}, corresponding to $C=C$ carbonyl groups, suggesting no chain scission or severe degradation occurred, or any degradation was too minor to produce detectable isolated carbonyl groups [19].

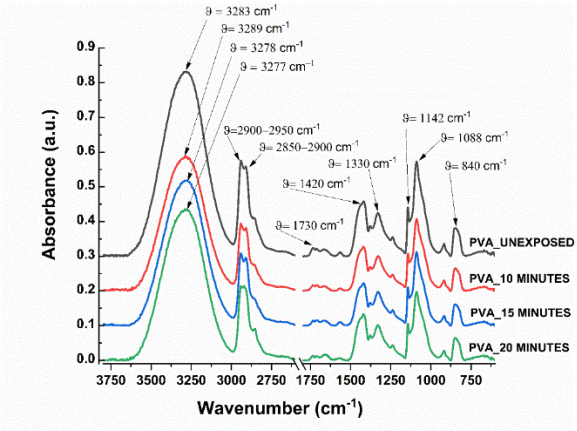

Fig. 2. ATR-FTIR spectra of films prepared from unexposed and UV-irradiated PVA solutions (UV intensity was 9.62 mW/cm² for all irradiated samples and the corresponding doses: 0, 5.77, 8.66, and 11.54 J/cm²).

According to Nagura et al. [20], shifts in the OH stretching peak ($\upsilon = 3300\ cm^{-1}$) and changes in the intensity of the peak at 864 cm^{-1} provide insight into the syndiotactic and isotactic structures of PVA films. A shift to higher frequencies indicates weakened intermolecular hydrogen bonds and reduced

syndiotacticity, with strengthened intramolecular hydrogen bonds forming within isotactic sequences. Conversely, a shift to lower frequencies suggests increased intermolecular hydrogen bonds between syndiotactic sequences, leading to denser molecular packing, restricted molecular motion [20], and a decreased degree of crystallinity [21].

In Fig. 2, the wavenumber of the maximum OH stretching absorption is noted for each spectrum and shifts with UV exposure, reflecting structural changes in the crystalline regions of PVA [20]. For 10 minutes of UV exposure, the peak shifts to a higher wavenumber compared to unexposed films and those exposed for 15 and 20 minutes, indicating the formation of intramolecular hydrogen bonds within isotactic sequences. In contrast, 15 and 20 minutes of UV exposure result in a lower-wavenumber shift, suggesting intermolecular hydrogen bonds between syndiotactic sequences.

To quantify the effects of UV exposure, the peak areas of major ATR-FTIR bands were calculated: $C-H$ stretch ($\upsilon = 2850-2950\ cm^{-1}$, $A_{CH\ stretch}$), $C=O$ stretch ($\upsilon = 1730\ cm^{-1}$, $A_{C=O}$), $C-H$ bending vibration of the CH_2 groups ($\upsilon = 1420\ cm^{-1}$, $A_{C-H\ from\ CH_2}$), and $C-O$ stretch in $CH(OH)$ ($\upsilon = 1088\ cm^{-1}$, $A_{C-O\ in\ CH(OH)}$). These were divided by the peak area of the OH stretch ($\upsilon = 3300\ cm^{-1}$, A_{OH}) to normalize against hydroxyl variations and avoid misinterpretation of photooxidation due to absorbed water [22]. The resulting ratios, multiplied by 100 and expressed as percentages, are presented in Table 1 for different UV exposure times. The corresponding doses are calculated as intensity multiplied by exposure time (seconds).

Table 1

Ratios of ATR-FTIR Peak Areas to OH Stretching Peak Area as a Function of UV Exposure Time and Doses Calculated for a Constant Intensity ($9.62\ mW/cm^2$)

Ratios (%)	UV Exposure Time (min.)	0	10	15	20
	Dose (J/cm^2)	0	5.77	8.66	11.57
$R1 = A_{\text{CH stretch}}/A_{OH}$		8.0669	7.9826	7.8254	7.7193
$R2 = A_{\text{C=O}}/A_{OH}$		0.0797	0.1465	0.0701	0.0564
$R3 = A_{\text{C–H from CH2}}/A_{OH}$		4.7898	4.3449	4.4917	4.4794
$R4 = A_{\text{C–O in CH(OH)}}/A_{OH}$		7.5394	7.7468	6.5247	7.3951

3.2. Morphological Aspects and Contact Angle Measurements of UV-Exposed PVA Films

Surface Morphology: The surface morphology of cast polyvinyl alcohol (PVA) films, prepared from UV-irradiated aqueous solutions, was analysed using Scanning Electron Microscopy (SEM), with results presented in Fig. 3.

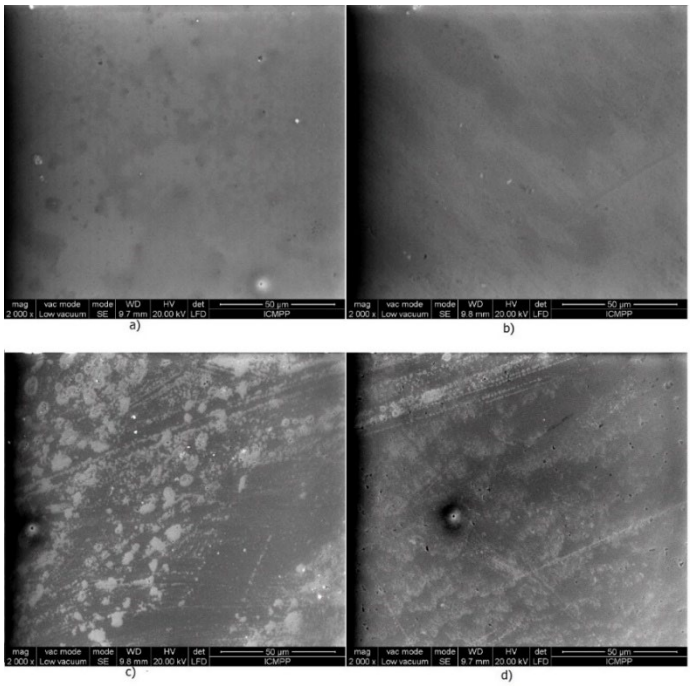

Fig. 3. SEM images of PVA films: (a) before UV exposure, (b) after 10 min, (c) after 15 min, and (d) after 20 min of UV exposure (constant intensity of 9.62 mW/cm^2; doses: 0, 5.77, 8.66, and 11.54 J/cm^2, respectively).

Pristine (unexposed) PVA films exhibit a smooth, uniform surface characterized by small, evenly distributed granular formations. These granules likely arise from incomplete polymerization of vinyl acetate or conformational variations in the polymer chains during film formation [23]. After 10 minutes of UV exposure, the film surface becomes noticeably smoother. This change is attributed to the formation of intramolecular hydrogen bonds, which facilitate tighter packing of PVA chains, enhancing the structural order of the polymer matrix [5, 20]. ATR-FTIR analysis supports this, showing a 5.6% increase in the R_4 ratio ($A_{\mathrm{C-O\ in\ CH(OH)}}/A_{OH}$) (Table 1), indicative of increased crystallinity due to ordered chain arrangements. Additionally, UV-induced photooxidation converts $CH(OH)$ groups to polar carbonyl ($C=O$) groups ($\upsilon = 1730\ cm^{-1}$) forming a hydrophilic surface layer [12]. This layer interacts with ambient moisture or residual water during drying, causing slight surface swelling that further smooths the film [24]. The smoother surface and enhanced polarity at 10 minutes are critical for applications requiring uniform surface properties, such as liquid crystal (LC) alignment. In contrast, films exposed to UV for 15- and 20-minutes show progressive surface irregularities (Figs. 2c, d). These changes result from crosslinking via ether ($C-O-C$) and ester ($-COO-$) bridges, which replace hydrogen bonds and increase network rigidity [7-9, 22]. The ATR-FTIR data indicate a $1-3\%$ reduction in R_4 ratio at these exposure times, reflecting a

decrease in crystallinity due to the formation of covalent bridges that disrupt chain mobility. The altered surface morphology reduces the accessibility of polar groups, impacting surface properties and optical performance, as discussed below.

Contact Angle and Surface Properties: Surface polarity (P) and free energy of hydration (ΔG_w) of PVA films were determined using contact angle measurements with water and diiodomethane, analyzed via the extended Fowkes theory and Young–Dupré equation [25]. The work of adhesion (W_a) was calculated using Equation (3):

$$W_a = \gamma_l(1 + cos\,\theta) \quad (3)$$

where θ is the contact angle of the test liquid and γ_l is the liquid surface tension.

Additionally, W_a was expressed as:

$$W_a = 2\sqrt{\gamma_l^d \gamma_s^d} + 2\sqrt{\gamma_l^p \gamma_s^p} \quad (4)$$

with γ_l^d and γ_l^p as dispersive and polar components of the liquid surface tension, and γ_s^d and γ_s^p as those of the solid surface energy [26].

Surface polarity (P) was calculated as: $P = \gamma_s^p/\gamma_s = \gamma_s^p/(\gamma_s^d + \gamma_s^p)$ (Equation 5) and ΔG_w was derived from Equation (6):

$$\Delta G_w = -\gamma_l(1 + \cos\theta_w) \quad (6)$$

using the water surface tension ($\gamma_l = 72.8\,mN/m$). Surfaces with $\Delta G_w < -72.8\,mJ/m^2$ are hydrophilic [26]. Results are shown in Table 2.

Table 2.

Water (θ_w) and Diiodomethane (θ_D), Surface Polarity (P) and Surface Free Energy of Hydration (ΔG_w) of PVA Films Prepared from UV-Irradiated Solutions for a Constant Intensity ($9.62\,mW/cm^2$)

UV Exposure Time (minutes)	Dose (J/cm^2)	Water Contact Angle, θ_w (Degree)	Diiodomethane Contact Angle, θ_D (Degree)	Surface Polarity, P (%)	Surface Free Energy of Hydration, ΔG_w (mJ/m^2)
0	0	61.1±0.71	39.4±0.57	22.9±0.79	-108.09±0.79
10	5.77	45.8±0.53	42.7±0.52	35.6±0.62	-123.48±0.48
15	8.66	67.8±0.72	56.8±0.46	27.9±1.05	-100.66±0.85
20	11.57	71.5±0.61	59±0.76	26.0±1.02	-96.13±0.73

At 10 minutes of UV exposure, films exhibit peak surface polarity ($P = 35.61 \pm 0.62\%$) and wettability ($\Delta G_w = -123.48\,mJ/m^2$) driven by photooxidation that cleaves $C-H$ and $C-OH$ bonds, forming polar $C=O$ and hydroperoxide ($C-OOH$) groups. ATR-FTIR data show increased R_2 ($A_{C=O}/A_{OH}$) and R_4 ($A_{C-O\text{ in }CH(OH)}/A_{OH}$) ratios, with a higher-wavenumber shift in the OH stretching peak ($\upsilon = 3300\,cm^{-1}$), indicating intramolecular hydrogen bonding within isotactic sequences [20]. This ordered structure, combined with

polar group formation, reduces the water contact angle to $45.8 \pm 0.53°$, enhancing hydrophilicity and supporting applications requiring strong surface interactions, such as LC alignment.

For 15- and 20-minute UV exposures, surface polarity decreases ($P = 27.9 \pm 1.05\%$ and $26.0 \pm 1.02\%$, respectively) and contact angles increase ($\theta_w = 67.8 \pm 0.72°$and $71.7 \pm 0.61°$), reflecting reduced wettability ($\Delta G_w = -100.66 \pm 0.85$ and -96.13 ± 0.73 mJ/m^2). ATR-FTIR data show reduced R_2 and R_4, with a lower-wavenumber OH peak shift, suggesting intermolecular hydrogen bonding and crosslinking via ether and ester bridges [9, 26]. These covalent bonds form less polar $C-O-C$ linkages, reducing free OH and $C=O$ groups and increasing network rigidity, which limits polar group accessibility and decreases hydrophilicity.

The mechanism of UV radiation effects on PVA solutions, derived from these results, is consistent with that proposed by Vijayalakshmi et al. [9]. Initially, UV radiation excites and dissociates water, forming hydrogen and hydroxyl radicals. Hydroxyl radical abstract hydrogen from the polymer, followed by internal hydrogen transfer and intramolecular rearrangements. For short UV exposure (10 minutes), intramolecular OH bond formation and photooxidation occur. With prolonged exposure (15 and 20 minutes), OH bonds are reduced and replaced by ether and ester bridges. Chain scission may occur, but no severe degradation from oxidation of these fragments was detected.

Below is proposed a simplified reaction scheme summarizing the qualitative key chemical changes [7-9, 22]:

- Stage 1: Radical Formation:

$$H_2O \xrightarrow{UV} \cdot OH + \cdot H$$
$$-CH_2-CH(OH)- + \cdot OH \longrightarrow -CH\cdot -CH(OH)- + H_2O$$

- Stage 2: Photooxidation (10 Minutes):

$$-CH\cdot -CH(OH)- + O_2 \longrightarrow -CH(OOH)-CH(OH)-$$
$$\longrightarrow -C(=O)-CH(OH)- + H_2O$$

- Stage 3: Ether/Ester Formation (15–20 Minutes):

$$-CH(OH)-CH(OH)- \longrightarrow -CH(O-C)H- + H_2O$$
$$-CH(OH)- + -OCOCH_3 \longrightarrow -CH-O-C(=O)CH_3 + H_2O$$

Surface Polarity and Wettability of Stretched PVA Films: Contact angles of water and diiodomethane on cast and uniaxially stretched polyvinyl alcohol (PVA) films were measured using the sessile drop method to determine surface polarity (P) and surface free energy of hydration (ΔG_w). Measurements were conducted for films with UV exposure times of 0, 10, 15, and 20 minutes and stretching degrees (γ) of 1.5 and 2. P and ΔG_w were calculated, with results presented in Fig. 4. a (P) and Fig. 4. b (ΔG_w).

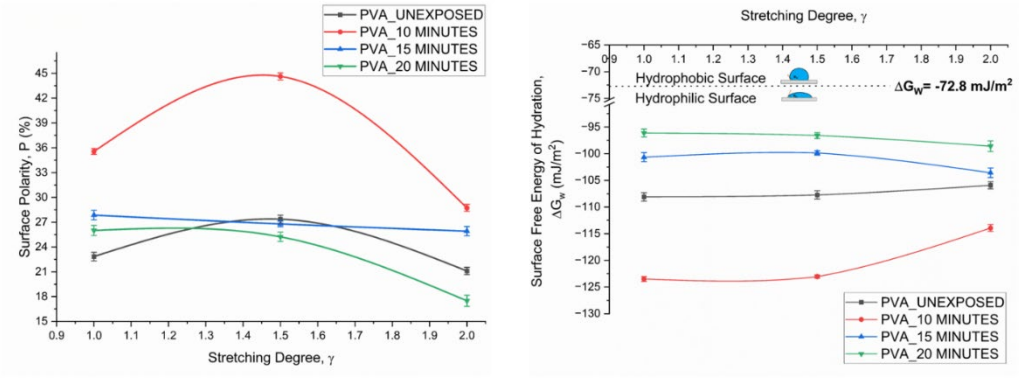

Fig. 4: (a) Surface polarity (P) and (b) Wettability (ΔG_w) as a function of UV exposure time and stretching degree (UV intensity was 9.62 mW/cm^2 for all irradiated samples and the corresponding doses: 0, 5.77, 8.66, and 11.54 J/cm^2).

Unstretched, unexposed films exhibit moderate polarity ($P = 22.8 \pm 0.52$ %) and wettability ($\Delta G_w = -108.09 \pm 0.79$ mJ/m^2, Table 2) due to randomly oriented OH groups. Stretching to $\gamma = 1.5$ aligns polymer chains, exposing more OH groups and increasing polarity ($P = 27.4 \pm 0.49\%$) and ΔG_w, reflecting enhanced hydrophilicity [24]. At $\gamma = 2$, excessive stretching buries polar groups, exposing non-polar $-CH_2-$ segments, reducing polarity ($P = 21.1 \pm 0.44\%$) and wettability.

For 10-minute UV-exposed films, photooxidation (Stage 2 of the degradation mechanism) forms $C = O$ and OH groups, yielding high polarity ($P = 35.6 \pm 0.35$ %) and wettability ($\Delta G_w = -123.48 \pm 0.48$ mJ/m^2) in unstretched films [7-9]. Stretching to $\gamma = 1.5$ maximizes polarity ($P = 44.6 \pm 0.42\%$) and G_w by aligning chains to enhance polar group exposure. At $\gamma = 2$, polarity drops to $P = 28.7 \pm 0.42\%$ as $-CH_2-$ groups dominate, reducing wettability.

Films exposed to UV for 15 and 20 minutes show decreased polarity $P = 27.9 \pm 1.05\%$ and $26.0 \pm 1.02\%$, respectively) and wettability in unstretched states due to crosslinking via ether ($C-O-C$) and ester ($-COO-$) bridges (Stage 3), which reduces OH and $C = O$ group availability [7-9]. Stretching these films further lowers polarity and ΔG_w, as cross-linked chains align to expose non-polar $-CH_2-$ groups, with $\gamma = 2$ showing the greatest reduction due to buried polar groups.

For 15-minute films, ΔG_w slightly increases at $\gamma = 1.5$ due to residual polar group alignment but decreases at $\gamma = 2$. For 20-minute films, ΔG_w consistently decreases with stretching due to the cross-linked, hydrophobic surface [12, 24]. All ΔG_w values remain below value of -72.8 mJ/m^2, indicating sustained hydrophilicity [25, 26]. The interplay of UV-induced photooxidation (enhancing

polarity at 10 minutes) and crosslinking (reducing polarity at 15–20 minutes) with stretching-induced chain alignment governs surface properties. Optimal polarity and wettability occur at 10 minutes UV and to $\gamma = 1.5$, driven by polar group exposure, while prolonged UV and higher stretching shift the surface toward hydrophobicity, impacting applications like liquid crystal alignment [24].

3.3. Induced Optical Birefringence of Cast and Uniaxially Stretched Polymer Films

The optical birefringence (Δn) of polyvinyl alcohol (PVA) films ($0.8 - 0.9\,mm$ thick), prepared from UV-irradiated aqueous solutions (0, 10, 15, 20 minutes) and uniaxially stretched to degrees ($\gamma = 1.5$ and 2), was measured and is presented in Fig. 5.

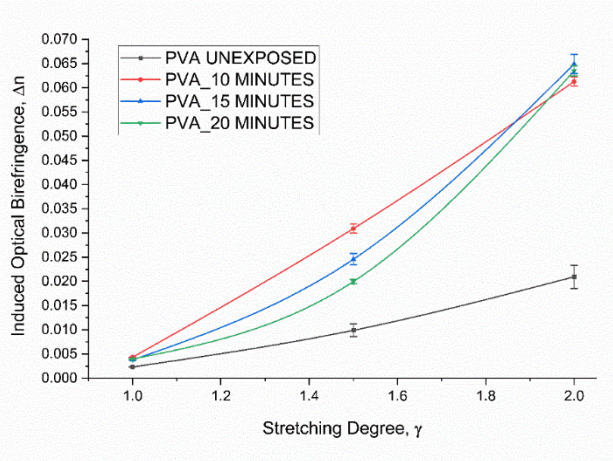

Fig. 5. Induced optical birefringence of PVA films as a function of stretching degree, γ, for different UV exposure times at a constant intensity of 9.62 mW/cm^2 (doses: 0, 5.77, 8.66, and 11.54 J/cm²).

Birefringence increases linearly with stretching for all samples, with UV-exposed films showing higher anisotropy than pristine ones. Stretching induces significantly greater birefringence ($\Delta n = 0{,}0209$ at $\gamma = 2$ for pristine films) than UV exposure alone ($\Delta n = 0.0023$ for unstretched pristine films).

Stretching aligns $-CH_2 - CH(OH) -$ chains, enhancing crystallinity and anisotropy [10]. For pristine films, birefringence rises from $\Delta n = 0.0023$ (unstretched) to 0.0099 ($\gamma = 1.5$) and 0.0209 ($\gamma = 2$). UV-exposed films exhibit higher baseline Δn due to pre-existing chain order from UV-induced modifications [20, 44]. At $\gamma = 1.5$, 10-minute UV-exposed films show the highest birefringence ($\Delta n = 0.03092 \pm 0.00092$), with a strictly linear dependence on γ, driven by flexible chains and intramolecular hydrogen bonding from photooxidation (Stage 2) [4, 7, 8, 20, 22]. This smooth, ordered matrix optimizes chain alignment at moderate stretching. At $\gamma = 2$, 15- and 20-minute UV-exposed films slightly

surpass ($\Delta n = 0.0649 \pm 0.00198$ and 0.06351 ± 0.00104 vs. 0.06128 ± 0.00093 for 10 minutes), showing slight deviation from linearity due to crosslinking (Stage 3) [7-9]. Crosslinking forms stiff ether ($C - O - C$) and ester ($-COO -$) bridges, limiting alignment at $\gamma = 1.5$ but sustaining it at $\gamma = 2$, where shorter chains align under higher strain [10, 11].

UV exposure enhances birefringence in unstretched films, peaking at 10 minutes ($\Delta n = 0.00434 \pm 0.000043$) compared to pristine ($\Delta n = 0.00232 \pm 0.000057$), 15-minute ($\Delta n = 0.00379 \pm 0.000082$, and 20-minute ($\Delta n = 0.00398 \pm 0.000111$) films. Hydroxyl radicals ($\cdot OH$) from UV exposure cleave long chains into shorter, mobile segments, which align during casting due to shear forces and compact into ordered domains during slow drying at $27°C$ [7-9, 27]. At 10 minutes, photooxidation forms polar $C = O$ and OH groups, enhancing chain mobility and dipole-driven alignment, increasing the extraordinary refractive index and Δn [10, 11]. At 15–20 minutes, crosslinking creates a denser, less flexible network, slightly reducing Δn compared to 10 minutes but still exceeding pristine films due to ordered covalent bridges [5, 8, 9].

The interplay of UV-induced chemical changes and stretching governs birefringence. At 10 minutes, intramolecular hydrogen bonding and photooxidation create a flexible, ordered matrix, optimizing Δn at $\gamma = 1.5$. Prolonged UV exposure (15–20 minutes) induces crosslinking, stiffening the network and limiting alignment at lower γ, but higher strain ($\gamma = 2$) overcomes this, enhancing anisotropy. Casting and drying further amplify Δn in UV-exposed films by promoting shear-induced and dipole-driven chain alignment [10, 27]. These findings highlight that 10-minute UV exposure with moderate stretching ($\gamma = 1.5$) maximizes birefringence for applications like polarizers, while longer exposures benefit from higher stretching to leverage crosslinking-induced order.

3.4. Alignment of 7 CB Liquid Crystal on the Surface of Cast and Uniaxially Stretched Films

The alignment of 7CB liquid crystal (LC) molecules on cast and uniaxially stretched polyvinyl alcohol (PVA) films, prepared from UV-irradiated aqueous solutions, was investigated using polarized optical microscopy (POM) under crossed polarizers (Fig. 6). Films were stretched at $42 - 45°C$ to degrees ($\gamma = 1.5$ and 2) to align polymer chains, enhancing structural order, optical anisotropy, and surface properties for LC alignment applications [10, 14]. Releasing a thin layer of 7 CB LC molecules onto the studied surface and analysing the images under crossed polarizers distinct bright and dark states were revealed. The contrast ratio ($R_{Bright/Dark}$), calculated from bright and dark state intensities (Equation 2), indicates the uniformity of 7CB orientation (Table 3).

LC Alignment and Surface Interactions: POM images (Fig. 6) show distinct bright and dark states, reflecting changes in light polarization as 7CB aligns

on anisotropic PVA surfaces. Rotating the film by 45° maximizes transmitted light intensity (bright state), while a 90° angle minimizes it (dark state), driven by the alignment of the 7CB director relative to the transmission axis of analyzer [12]. Stretching enhances surface anisotropy, promoting planar alignment of 7CB along the stretching direction via elastic and steric interactions [13].

The $R_{Bright/Dark}$ values increase with stretching, indicating improved alignment (Table 3). For pristine films (0 minutes), $R_{Bright/Dark}$ rises from 2.05 ± 0.08 (unstretched) to 3.91 ± 0.08 ($\gamma = 1.5$) and 4.77 ± 0.05 ($\gamma = 2$), reflecting increased chain alignment. Films exposed to UV for 10 minutes show optimal 7CB alignment, with $R_{Bright/Dark}$ peaking at 7.16 ± 0.05 ($\gamma = 1.5$) and 9.49 ± 0.06 ($\gamma = 2$), driven by high surface polarity ($P = 44.6 \pm 0.42\%$, Table 2) and birefringence ($\Delta n = 0.03092 \pm 0.00092$, Fig. 5) from photooxidation (Stage 2) [7, 8, 10]. The smooth surface (Fig. 3.b) and polar OH and $C = O$ groups enhance adhesion through dipole-dipole and hydrogen-bonding interactions with the $-CN$ group of 7CB, supporting uniform tilted anchoring [12, 15, 16]. At 15 minutes, alignment remains strong ($R_{Bright/Dark} = 7.79 \pm 0.11$R at $\gamma = 1.5$, 8.75 ± 0.09 at $\gamma =$), but crosslinking (Stage 3) reduces polarity ($P = 27.9 \pm 1.05\%$), weakening adhesion [7-9]. At 20 minutes, alignment decreases ($R_{Bright/Dark} = 6.68 \pm 0.04$ at $\gamma = 1.5$, and 8.55 ± 0.07 at $\gamma = 2$) due to lower polarity ($P = 26.0 \pm 1.02\%$) and surface irregularities (Fig. 3.d), though higher birefringence sustains moderate alignment at $\gamma = 2$ [10].

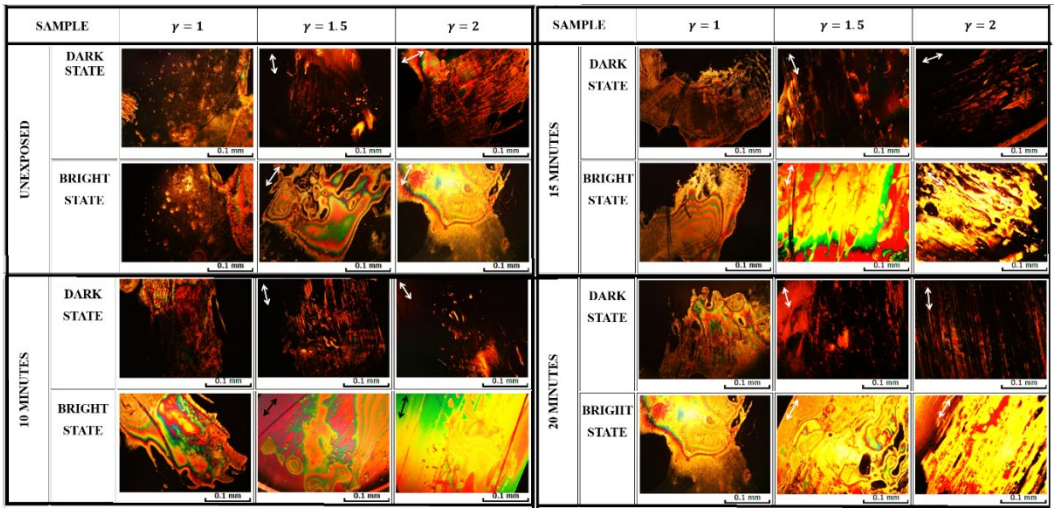

Fig. 6. POM images of cast and uniaxially stretched PVA films prepared from UV-irradiated solutions (doses: 0, 5.77, 8.66, and 11.54 J/cm²), covered with 7CB.

Table 3.

Contrast Ratios ($R_{Bright/Dark}$) of 7 CB on PVA Films.

UV Exposure Time (minutes)	Dose (J/cm^2)	$R_{Bright/Dark}$		
		$\gamma = 1$ (Unstretched)	$\gamma = 1.5$	$\gamma = 2$
0	0	2.05±0.08	3.91±0.08	4.77±0.05
10	5.77	4.87±0.11	7.16±0.05	9.49±0.06
15	8.66	4.10±0.22	7.79±0.11	8.75±0.09
20	11.57	2.73±0.07	6.68±0.04	8.55±0.07

Mechanistic Insights: 7CB alignment depends on surface polarity and anisotropy. At 10 minutes UV, photooxidation forms polar groups, increasing polarity and enabling strong adhesion via $-CN$ interactions, while moderate stretching ($\gamma = 1.5$) optimizes anisotropy ($\Delta n = 0.03092$) for planar alignment [13, 15]. Crosslinking at 15–20 minutes reduces polarity, limiting adhesion, but increased birefringence at $\gamma = 2$ ($\Delta n = 0.0649$ and 0.06351) supports alignment through elastic interactions [10]. Unstretched films show moderate alignment due to shear-induced chain order during casting and drying, enhanced by UV-induced chain scission and polar group formation [7, 8, 27]. The synergy of high polarity and moderate stretching at 10 minutes maximizes 7CB alignment, making these films ideal for LC displays and polarizers.

4. Conclusions:

This study elucidates the synergistic effects of UV irradiation (0, 10, 15, 20 minutes) and uniaxial stretching ($\gamma = 1.5$ and 2) on polyvinyl alcohol (PVA) films, optimizing their optical birefringence, surface polarity, wettability, and 7CB liquid crystal (LC) alignment for applications in polarizers and LC displays.

UV exposure induces a three-stage degradation mechanism: at 10 minutes, photooxidation (Stage 2) forms polar $C=O$ and OH groups, promoting intramolecular hydrogen bonding, a smooth surface (Fig. 3b), high polarity ($P = 35.6 \pm 0.62\%$, Table 2), and peak wettability ($\Delta G_w = -123.48 \pm 0.48\ \mathrm{mJ/m^2}$). These changes enhance chain mobility and alignment during casting, boosting birefringence ($\Delta n = 0.00434 \pm 0.000043$, Fig. 5) and 7CB alignment ($R_{Bright/Dark} = 4.87 \pm 0.11$, unstretched, Table 3). At 15–20 minutes, crosslinking via ether ($C-O-C$) and ester ($-COO-$) bridges (Stage 3) increases rigidity, introduces surface irregularities (Figs. 3c, d), and reduces polarity ($P = 26.0 - 27.9\%$) and wettability, slightly lowering birefringence ($\Delta n = 0.00379 - 0.00398$).

Stretching aligns polymer chains, linearly increasing birefringence (Fig. 5). At $\gamma = 1.5$, 10-minute UV-exposed films achieve peak birefringence ($\Delta n = 0.03092 \pm 0.00092$) and polarity ($P = 44.6 \pm 0.42\%$), inducing 7CB alignment in this non-confined configuration ($R_{Bright/Dark} = 7.16 \pm 0.05$) due to a flexible, ordered matrix and strong $-CN$ dipole interactions with polar groups. At $\gamma = 2$, 15- and 20-minute films show higher birefringence ($\Delta n = 0.0649 \pm 0.00198$ and

0.06351 ± 0.00104) and sustain 7CB alignment ($R_{Bright/Dark} = 8.75 \pm 0.09$ and 8.55 ± 0.07) despite reduced polarity, as crosslinking supports anisotropy under higher strain [20]. However, excessive stretching ($\gamma = 2$) at 10 minutes reduces polarity ($P = 28.7 \pm 0.42\%$) and wettability due to non-polar $-CH_2-$ exposure.

The interplay of surface polarity and anisotropy governs 7CB alignment. At 10 minutes and $\gamma = 1.5$, high polarity and moderate birefringence maximize adhesion and planar alignment via dipole-dipole and hydrogen-bonding interactions. Prolonged UV exposure reduces polarity, but stretching-induced anisotropy sustains alignment, particularly at $\gamma = 2$.

The findings of this study demonstrate that 10-minute UV exposure combined with moderate stretching ($\gamma = 1.5$) significantly enhances surface polarity, birefringence, and 7CB alignment in thick, non-confined layers. These results establish a foundation for further optimization using thin films and mechanical rubbing. These results advance polymer surface engineering, offering a versatile framework for designing sustainable, high-performance optical materials for photonic devices, such as polarizers, optical filters, and LC displays.

Acknowledgements

This work was supported by a National Research Grants of the Gheorghe Asachi" Technical University of Iași, Romania (TUIASI), project number: **GNaC 2023_264 /2024.**

REFERENCES

[1] *V. Pop, D.O. Dorohoi, E.A. Cringeanu*, New method for determining birefringence dispersion, J. Macromol. Sci.-Phys. B, Vol. **33**, Iss. (3&4), 1994, https://doi.org/10.1080/00222349408248099.

[2] *M.H. Han, J.K. Shin, K.I. Oh, Y.J. Lee, D.H. Song et al*., Preparation of recycled poly (vinyl alcohol) (PVA)/iodine polarizing film, Polym. Polym. Compos., Vol. **18**, Iss. 7, 2010, https://doi.org/10.1177/0967391110018007.

[3] C*.D. Nechifor, E. Angheluta, D.O. Dorohoi*, Birefringence of etired poly (vinyl alcohol) (PVA) foils, Mat. Plast., Vol. **4**, Iss. 2, 2010.

[4] *C.D. Nechifor, C.B. Zelinschi, D.O. Dorohoi*, Influence of UV and Gamma radiations on the induced birefringence of stretched poly(vinyl) alcohol foils. J. Mol. Struct., Vol. **1062**, 2014, https://doi.org/10.1016/j.molstruc.2014.01.011.

[5] *C.D. Nechifor, M. Aflori, D.O. Dorohoi*, Anisotropy of thin foils obtained from microwave-irradiated poly (vinyl alcohol) aqueous solutions. Polymers, Vol. **11**, Iss. 6, 2019, https://doi.org/10.3390/polym11061072.

[6] *C.D. Nechifor, M. Postolache, R.M. Albu, A.I. Barzic, DO Dorohoi*, Induced birefringence of rubbed and stretched polyvinyl alcohol foils as alignment layers for nematic molecules, Polym. Adv. Technol., Vol. **30**, Iss. 8, 2019, https://doi.org/10.1002/pat.4647.

[7] *N.S. Allen, M. Edge*, Fundamentals of Polymer Degradation and Stabilization, Springer, London, 1992.

[8] *D. Hamad, M. Mehrvar, R. Dhib*, Experimental study of polyvinyl alcohol degradation in aqueous solution by UV/H_2O_2 process, Polym. Degrad. Stab., Vol. **103**, 2014, https://doi.org/10.1016/j.polymdegradstab.2014.02.018
[9] S.*P Vijayalakshmi, G. Madras*, Photodegradation of poly (vinyl alcohol) under UV and pulsed-laser irradiation in aqueous solution, J. Appl. Polym. Sci., Vol. **102**, Iss. 2, 2006, https://doi.org/10.1002/app.23736
[10] *I.M. Ward*, Structure and Properties of Oriented Polymers, Springer, Dordrecht, 1997, https://doi.org/10.1007/978-94-011-5844-2
[11] *M. Postolache, D.G. Dimitriu, C.D. Nechifor, S Condurache Bota, V. Closca, D.O. Dorohoi*, Birefringence of thin uniaxial polymer films estimated using the light polarization ellipse, Polymers, Vol. **14**, Iss. 5, 2022, https://doi.org/10.3390/polym14051063.
[12] *J.A. Castellano*, Surface anchoring of liquid crystal molecules on various substrates, Mol. Cryst. Liq. Cryst., Vol. **94**, Iss. 1-2, 1983, https://doi.org/10.1080/00268948308084245.
[13] *P.G. de Gennes, J. Prost*, The Physics of Liquid Crystals, Oxford University Press, Oxford, 1993, https://doi.org/10.1093/oso/9780198520245.001.0001.
[14] D.W. Berreman, Alignment of liquid crystals by grooved surfaces, Mol. Cryst. Liq. Cryst., Vol. **23**, Iss. 3-4, 1973, https://doi.org/10.1080/15421407308083374.
[15] *J. Cognard*, Alignment of nematic liquid crystals and their mixtures, Gordon and Breach Science Publishers, 1982.
[16] I. Dierking, Textures of Liquid Crystals. Wiley, Darmstadt, 2003, https://doi.org/10.1002/3527602054.
[17]***W.S. Rasband*, ImageJ User Guide. National Institutes of Health, 2012, https://imagej.nih.gov/ij/docs/guide/.
[18] *J. Coates*, Interpretation of Infrared Spectra, A Practical Approach. In: (Meyers RA ed.) Encyclopedia of Analytical Chemistry, Wiley, Chichester, 2000.
[19] *A. Bernal, I. Kuritka, V. Kasparkova, P. Saha*, The effect of microwave irradiation on poly (vinyl alcohol) dissolved in ethylene glycol, J. Appl. Polym. Sci., Vol. **128**, Iss. 1, 2013, https://doi.org/10.1002/app.38133.
[20] *M. Nagura, S. Matsuzawa, K. Jamaura, H. Ishikawa*, Tacticity dependence of molecular motion in crystal of poly (vinyl alcohol), Polym. J., Vol. **14**, Iss. 1, 1982, https://doi.org/10.1295/polymj.14.69.
[21] *K. Sugiura, M. Hashimoto, S. Matsuzawa, K. Yamaura*, Influence of degree of crystallinity and syndiotacticity on infrared spectra of solid PVA, J. Appl. Polym. Sci., Vol. **82**, Iss. 5, 2001, https://doi.org/10.1002/app.1963.
[22] *J.F. Rabek*, Polymer Photodegradation: Mechanisms and Experimental Methods. Chapman & Hall: London, 1995, http://dx.doi.org/10.1007/978-94-011-1274-1.
[23] *C.B. Zelinschi, I. Stoica, D.O. Dorohoi*, Changes in morphology and optical properties of polyvinyl alcohol foils induced by Congo red dye concentration and stretching degree, J. Polym. Eng., Vol. **34**, Iss. 3, 2014, https://doi.org/10.1515/polyeng-2013-0189.
[24] *K.T. Hong, H. Imadojemu, R.L. Webb*, Effects of oxidation and surface roughness on contact angle, Exp. Therm. Fluid Sci., Vol. **8**, Iss. 4, 1994, https://doi.org/10.1016/0894-1777(94)90058-2.
[25] *C. J. Van Oss*, Interfacial Forces in Aqueous Media. CRC Press, Boca Raton, 1994.
[26] *D.H. Kaelble*, Dispersion-polar surface tension properties of organic solids, J. Adhes., Vol. **2**, Iss. 2, 1970, https://doi.org/10.1080/0021846708544582.
[27] *W.M. Jr. Prest, D.J. Luca*, The origin of the optical anisotropy of solvent cast polymeric films, J. Appl. Phys.,Vol. **50**, Iss. 10, 1979, https://doi.org/10.1063/1.325795.